

# Tissue Slices in the Study of Lung Metabolism and Toxicology

by Bruce A. Freeman\* and John J. O'Neil†

Lung tissue slices are model systems for the study of pulmonary metabolism. Because of the speed and simplicity of slice preparation, lung slices have been used in studies of oxygen, amino acid, carbohydrate and lipid utilization and adenine nucleotide metabolism. Dose-response characteristics for toxicants are readily described because multiple lung samples can be studied from the same animal or a population of animals. Lung slices prepared from animals exposed to oxidant air pollutants exhibit alterations in respiration, glucose consumption and lipid metabolism. These studies have indicated both direct toxic effects of air pollutants on enzyme systems and also air pollutant-induced changes in the cellularity of lungs.

## Introduction

Lung tissue slices are one of a variety of *in vitro* techniques which are used to study lung cellular biology and nonrespiratory lung function. These techniques also include lung subcellular fractions, homogenates, homogenous populations of isolated or cultured cells, mixed cell organ cultures, and the isolated and perfused lung.

*In vivo* studies of lung metabolism and toxicology are complicated because of the small relative mass of lung tissue (about 1% of total body mass) and an enormous relative blood flow (normally the entire cardiac output). These combine to produce exceedingly small changes in the arteriovenous difference of most circulating metabolites. For example, efforts to measure lung glucose consumption *in vivo* are impractical due to an inability to measure small arteriovenous blood glucose content differences precisely (1). *In vivo* lung toxicology studies are also rendered complex by systemic influences, including infiltration of phagocytic cells and the formation of immune complexes at the site of injury (2), which may, in their own right, mask attempts to alter the biochemical parameters under study.

Tissue slices are a useful *in vitro* tool for studying lung metabolism because of the speed and simplicity of slice preparation. Following slicing, several samples taken from the same lung may be studied simultaneously. This eliminates many experimental variations, and may

allow the assessment of metabolic alterations following lung injury or stress occurring *in vivo*. Dose-response curves of lung slice metabolism may also be generated by varying concentrations of an agent added to incubation mixtures in flasks which contain tissue from the same lung. Morphological and cellular integrity can also be maintained in tissue slices with minimal loss of metabolic activity. Cultured and isolated lung cells could be used to determine if tissue metabolic processes are unique to specific lung cell types and represent the sum of individual reactions of constituent cell types or, more likely, reflect a concerted response due to interactions between heterogeneous cell types (3). However, when using cultured or isolated cells, an absence of cell-cell and cell-matrix interactions may result in a loss of differentiated functions. *In vivo* metabolism may be mimicked by lung slices and can represent the composite metabolic activity of the several cell types which make up lung parenchyma.

Examples of lung metabolic activities which have been studied using lung slices include oxygen consumption (4,5) and the uptake and metabolism of amino acids (6), carbohydrates (1) and lipids (7). These activities are extremely stable for extended periods of time and, considering that the lung slice represents organized viable tissue, the measured metabolic activity probably represents normal enzymatic processes. Lung tissue slices seem to be unique among organs in their metabolic stability. For example, ATP levels in rat lung slices are constant for at least 1 hr of incubation and are identical to the ATP content of a rat lung flash-frozen *in situ* (8). The rate of incorporation of <sup>14</sup>C-labeled precursors into lung slice phosphatidylcholine remains constant for at least 2 hr (9). In fact, virtually every measurement of intermediary metabolism, which we

\*Division of Allergy, Respiratory, and Critical Care Medicine, Duke University Medical Center, Durham, NC 27710.

†Clinical Research Branch, Inhalation Toxicology Division, Health Effects Research Laboratory, U. S. Environmental Protection Agency, Research Triangle Park, NC 27711.

have made for extended periods with lung slices, proceeded in a linear fashion for up to 5 hr. This included glucose consumption, oxygen consumption, lactate production and oxidation of  $^{14}\text{C}$ -alanine (J. O'Neil, R. Slade and F. Englebrecht, unpublished observations). In contrast, Krebs measured the adenine nucleotide levels in rat liver slices and reported a precipitous (72%) and irreversible fall minutes after preparation of the slices (10).

A better understanding of nonrespiratory lung function through the use of lung tissue slices will expand our insight into both toxicological processes and clinical disorders. Physiological and morphological alterations are a consequence of advanced pathologic events at a molecular level. Thus, biochemical changes measurable with lung slices can be potentially the most sensitive early indicator of lung injury. For many metabolic measurements, tissue slices are equivalent to the more complicated isolated perfused lung preparation. Because they are relatively inexpensive and because it is easy to study large sample numbers, tissue slices are an attractive technique for measuring lung metabolism.

## Preparation of Tissue Slices

Lung slices used for metabolic studies should be prepared in a manner which minimizes tissue damage and maximizes accurate measurements of metabolic processes. It has not always been possible to extract an accurate description of techniques used in the preparation and incubation of tissue slices from information provided in published reports from different laboratories. Table 1 gives a list of items that are important to mention when describing experiments utilizing tissue slices. Critical factors which should be considered and described when reporting data include choice of incubation medium, slice thickness, mass of tissue assayed

and other incubation conditions such as temperature, head space gas concentrations and how the tissue was agitated in the medium.

## Anesthesia

Anesthetic residue may influence tissue metabolism. Intraperitoneal injection of sodium pentobarbital (100 mg/kg body weight) has been used, but pentobarbital may persist in the tissues and affect metabolism. Cervical dislocation leaves no anesthetic residue, but is followed by a massive neuronal discharge which may also affect lung metabolism. Halothane has been used (1) on the assumption that the halothane will ultimately be redistributed according to its partition coefficient and that the minimal residuum would have negligible influence on pulmonary metabolism. We have found pentobarbital injection and cervical dislocation of rats to have no significantly different effects on lung tissue glucose and oxygen metabolism.

## Slice Preparation

Following anesthesia the abdomen is opened, and the inferior vena cava and aorta are severed to reduce vascular blood volume. After approximately 30 sec, the thorax is opened with a midline incision and the heart and lungs are removed *en bloc*. Each lobe can then be dissected at the hilus, blotted lightly on cotton gauze to remove clots or debris adhering to the pleural surface and total lung mass determined.

It is difficult to prepare identical evenly cut free hand slices of lungs owing to the compliant and fibrous nature of this organ. Slices prepared free hand are usually of undetermined thickness. The Stadie-Riggs tissue slicer (Arthur Thomas Inc.) (11) will cut slices of a 0.5 mm nominal thickness; however, they tend to be uneven, may be damaged and are metabolically less active than lung slices produced by other methods (12,13). In addition, preparation of slices with this apparatus is time consuming and tedious. Uniform slices of lung tissue of thicknesses up to 1.0 mm can be rapidly made with the McIlwain tissue chopper (Brinkmann Instruments Inc.). They have been used successfully by several investigators (1,14) and seem to achieve optimum results in metabolic studies.

If one wishes to free the lung of blood before preparation of slices, an appropriate buffer can be perfused via the pulmonary artery before the lungs are removed from the thorax. Great care must be exercised because perivascular and interstitial edema can be induced by perfusion. Perfusion pressure must be kept to a minimum. If pulmonary edema occurs as a consequence of high perfusion pressure, this could lead to an underestimation of the actual tissue mass used in a study. If air is introduced with the perfusate into the pulmonary capillary bed, it will produce emboli which will block vessels and leave sections of the lung unperfused.

Table 1. Useful information to report regarding the use of tissue slices.

	Information
Animals	Species Age/weight Fed/fasted
Anesthesia	Drug Dose
Slice preparation	Method of slice preparation Thickness
Medium	Buffer Substrates Volume used
Incubation conditions	Weight of tissue slices incubated Stirring or shaking frequency Head space or dissolved gas concentrations Temperature Duration of incubation

Lung removal and slice preparation time must be minimized, since delay may result in irreversible alterations in cellular metabolism (5) if anoxia or substrate depletion occurs. Once tissue slices are prepared, they should not be blotted on absorbent paper or immersed in buffer. Blotting will dehydrate the tissue, causing underestimation of tissue mass. Immersion in buffer will fill the spongelike air spaces with liquid, causing overestimation of tissue mass. Such measurement errors may result in differences of 17 to 33% in calculations of lung metabolic activity (5). During preparation and handling of lung slices, we have found it convenient to keep the slices on nonabsorbent plastic disks, such as those supplied with the McIlwain tissue slicer. This had led to consistent and reproducible estimates of lung mass.

Once the tissue slices have been prepared, we routinely distribute the slices into separate piles. The hilar region of the lungs contains more large airways and vessels than parenchyma; hence, we have attempted to make each pile as heterogeneous as possible by assigning each slice sequentially to a different pile. Tissue mass can be estimated several ways. We have found it convenient to place a plastic disk with the piles of tissue onto an electronic balance with an automatic zero and to estimate the mass of tissue weight loss as each pile is removed.

Several simultaneous metabolic determinations may be made using tissue slices from the same lung. When measurements from more than two animals are performed, statistical analysis is possible. Use of duplicate or multiple flasks studied under similar conditions will increase the accuracy of a measurement. Toxicological dose-response studies of tissue slice metabolism can also be performed using multiple slice preparations from several animals. If multiple determinations are made on one animal's lungs,  $n$  should still be considered to be unity for statistical purposes.

## Tissue Slice Incubation Media

Phosphate or bicarbonate buffering solutions have been used for most studies on the metabolism of lung tissue slices. Measurements of  $\dot{Q}_{O_2}$  are usually done in the complete absence of  $CO_2$  and in this case, Krebs-Ringer phosphate has been used because it does not contain  $CO_2$  or  $HCO_3^-$ . Any  $CO_2$  produced can be absorbed with KOH (or a similar base). The estimation of  $\dot{Q}_{O_2}$  is therefore a direct measurement of volume change (15). Most studies on intermediary metabolism of lung slices (e.g., oxidation of  $^{14}C$ -labeled substrates, glucose utilization, lactate/pyruvate ratios, etc.) have been performed using Krebs-Ringer bicarbonate buffer because this solution more closely resembles the physiologic aqueous milieu. The use of bicarbonate buffers requires some care since  $CO_2$  goes into solution very slowly, especially in the absence of carbonic anhydrase, and equilibration with  $CO_2$  can take a long time (up to 1 hr). Conversely, when exposed to air, a

saturated solution will lose  $CO_2$  rapidly. Either bicarbonate or phosphate-buffered incubation media will buffer at pH 7.4 (16).

The substrate composition of the incubation medium will also affect the metabolism of lung slices (17); however, this can be used to good advantage when studying certain metabolic pathways or activities.

## Lung Slice Thickness

The cut face of a tissue slice will contain many damaged cells. However, as slice thickness is increased, the proportion of damaged cells will decrease and have a less significant influence on total slice metabolism. Unfortunately, as slice thickness increases, diffusion pathways are also lengthened. This can result in suboptimal metabolism because substrate delivery and gas diffusion may be rate limiting. Since alveoli fill with medium, exchange processes are also likely to occur from the air spaces to the tissue. Thus the diffusion distances for dissolved substrates in lung slices may be shorter than in a solid tissue such as liver or brain. Lung tissue slices function well at thicknesses above the optimal 0.7 mm which is predicted by the Warburg equation (15). Indeed,  $\dot{Q}_{O_2}$  and glucose oxidation proceeded at faster rates in 1.0 mm thick slices compared to slices less than 0.5 mm thick (12,14,18), suggesting that there is significant damage in the thinner slices. An investigator is faced with the necessity to minimize the contribution of cell damage and maximize the diffusion of substrates, when establishing tissue slice thickness and incubation conditions. For most studies, 1.0 mm tissue slices are of optimum thickness, although the metabolism of thicker slices has not been examined.

The local  $P_{O_2}$  in a tissue slice, which is affected by both slice thickness and the dissolved  $P_{O_2}$  of the incubation medium, is critical and may limit other metabolic processes. Oxygen gradients can exist both within single cells and throughout a tissue slice (19,20). This is because local  $P_{O_2}$  falls as cells undergo oxidative metabolism and an oxygen diffusion gradient will be established which is limited at three sites: (1) the surface boundary between the gas phase and the incubation medium (such as would exist in a manometer flask); (2) through the bulk phase of the incubation medium; and (3) through the tissue slice itself. Both the shaking rate during a manometric  $\dot{Q}_{O_2}$  determination and the rate of stirring when  $\dot{Q}_{O_2}$  is measured polarographically will affect the maximum  $\dot{Q}_{O_2}$  which can be measured. For manometric determinations, the shaking rate will affect the rate which oxygen dissolves in the incubation medium (16). The gas at the surface boundary is changed more often at higher shaking rates, resulting in a greater transfer of gas to the medium. We have observed that for manometric measurements, a shaking rate of 120 strokes/min maintained a maximal and constant  $\dot{Q}_{O_2}$  when using up to 100 mg of 1.0 mm thick rat lung slices and a head space gas of  $\geq 95\%$  oxygen (5). Decreasing the shaking rate below 120

strokes/min produced a fall in  $\dot{Q}_{O_2}$ . If increased amounts of tissue are put in the reaction flask, it may be necessary to agitate at a faster shaking rate to supply adequate amounts of oxygen. Similar arguments presumably apply for intermediary metabolism studies done in center well flasks although we are not aware that this relationship has been studied or reported.

It has been suggested that both the amount of oxygen available and the oxygen transfer rate potentially limit the rate of biological reactions in the Warburg manometric system (21). This observation can be confirmed in several ways. When the  $\dot{Q}_{O_2}$  of lung slices (40 mg) is measured in a 1.5 mL polarograph cell, the stirring rate must be 2 to 3 spinbar revolutions/sec or greater. Since there is no headspace gas in a polarograph cell, gas transfer into the medium is not a consideration, yet this rapid stirring rate must be maintained so that oxygen remains evenly distributed throughout the bulk phase of the medium and optimally diffuses into the tissue slice. Also, in 1.0 mm thick lung slices, the maximum  $\dot{Q}_{O_2}$  obtained occurs at dissolved oxygen concentrations of 40 to 60% or greater (Table 2), indicating that oxygen diffusion through the tissue slice will limit oxygen utilization at a low  $P_{O_2}$ .

We have also observed that the lactate production in 1.0 mm thick lung slices shaken at 120 strokes/min in a center well flask doubles when the headspace gas is 20% oxygen rather than 95% oxygen (5). This implies that a decreased oxygen gradient limits oxidative metabolism under these conditions. With a similar lung slice model, Montgomery et al. (14) report that  $^{14}C$ -acetate incorporation into fatty acids was reduced when 20% oxygen was used when compared to studies performed at 100% oxygen. However, when thinner slices were used, no difference in acetate incorporation was observed between air or oxygen. In this situation, substrate delivery was probably adequate, but oxygen availability may have been limited due to longer perfusion pathways which in turn inhibited acetate utilization.

## Lung Slice Mass

Knowledge of the mass of tissue used in a flask provides a reference for expressing the metabolism of lung tissue. Wet weight measurements are convenient, useful and avoid some potential pitfalls when using other denominators of lung metabolism (e.g., protein mass). Because of the variation which the fluid content of the lung can introduce into wet weight measurements, the metabolic activity of a weighed lung slice many times is best expressed in terms of the whole lung. For example, 100 mg of edematous lung tissue slices will contain less metabolically active tissue than a similar mass of normal lung. However, if the mass of the lung is known, metabolism can be expressed on a per lung basis. Useful comparisons can be made with this information. Expression of lung metabolic processes in terms of at least two denominators such as "whole lung" and "mg lung DNA" may be the most informative.

Table 2. Oxygen consumption of rat lung tissue slices.

Condition	$\dot{Q}_{O_2}$ , μmole/min per lung <sup>a</sup>
Polarographic measurement	
5% O <sub>2</sub>	0.41 ± 0.04
20% O <sub>2</sub>	1.18 ± 0.07
40% O <sub>2</sub>	1.58 ± 0.09
60% O <sub>2</sub>	1.69 ± 0.10
75% O <sub>2</sub>	1.72 ± 0.09
95% O <sub>2</sub>	1.79 ± 0.05
60% O <sub>2</sub> + 1mM KCN	0.24 ± 0.02
Manometric measurement	
95% O <sub>2</sub>	1.61 ± 0.13 <sup>b</sup>

<sup>a</sup>Mean ± SEM, n = 7. Rat lungs removed from 300–350 g male rats which weighed 1.39 ± 0.02 g were analyzed.

<sup>b</sup>Calculated from data of O'Neil et al. (5) using an estimated lung weight of 1.2 g.

The use of lung tissue slices presents some special problems if metabolic rates are expressed on the basis of the amount of DNA or protein present. During incubation, the air spaces will fill with fluid and tissue protein content will be overestimated if the slices are analyzed after incubation in a medium which contains protein. Conversely, if a protein-free incubation medium is used, extracellular protein (e.g., serum albumin and lipoprotein) may be diluted by the buffer. In addition, as the incubation flask is agitated, cellular fragments are lost into the medium which may be difficult to recover at the termination of the experiment. This loss of tissue during incubation will also confound dry weight estimates of tissue following incubation. Care must be taken in interpreting results derived from tissue slices because of possible differences from intact lung. For example, most neural and humoral controls are lost. These processes may participate in various metabolic functions including the control of pulmonary surfactant secretion (22,23). Also, fluid-filled alveolar spaces in tissue slice incubations provide alternative routes of substrate delivery to lung cells compared to those routes available *in vivo* or in isolated and perfused lung preparations. Substrate delivery from the alveolar space may also subvert possible important substrate modification processes since bloodborne substrates normally cross into the lung via the pulmonary capillary endothelium and interstitium.

## Measurement of Oxygen Consumption in Tissue Slices

### Manometric

Manometric measurements of tissue slice oxygen consumption are commonly performed using a Warburg manometer, named after the investigator who popularized the principle of its use. Respirometry is based on the principle that at constant temperature, any evolution or consumption of gas can be measured by

changes in its volume or pressure, according to the ideal gas law:

$$PV = nRT = P'V' \quad (1)$$

where  $n$  is the number of moles of gas present and  $R$  is the gas constant. We use the submarine all-glass volumometer (Gilson Medical Electronics, Inc., Middleton, WI) which is basically a reaction flask (containing medium and tissue) and a reference flask which are connected by a manometer, to indicate pressure differences between the two flasks. The reaction flask is connected to a micrometer calibrated in  $\mu\text{m}$  which, when turned, moves a small rod into the headspace of the reaction flask to replace the volume of oxygen removed by tissue metabolism (Fig. 1). Thus, manometric measurements of  $\dot{Q}_{\text{O}_2}$  are based on pressure decreases in the reaction flask due to oxygen utilization by tissue metabolism.  $\text{CO}_2$  can be adsorbed by an alkali placed on a piece of filter paper in the center well; thus any pressure change in the reaction flask is due to oxygen consumption by the tissue. A light coat of stopcock grease applied to the top of the center well will prevent the alkali from moving into the outer well by capillary action. We apply the grease from the end of a small rubber cork which is inserted through the neck of the reaction flask.

We have found that 60 to 90 mg of lung slices is a useful tissue weight for manometric  $\dot{Q}_{\text{O}_2}$  analysis. Following placement of tissue slices in the outer well of a flask which contains buffer, gas in the headspace is exchanged for 10 to 15 min with 100%  $\text{O}_2$ . This may be done while the flask is attached to the respirometer, submerged and shaking in the temperature bath. The flow rate and time of gassing needs to be decided empirically, knowing that under optimum conditions, 10 volumes of gas will displace approximately 99% of the

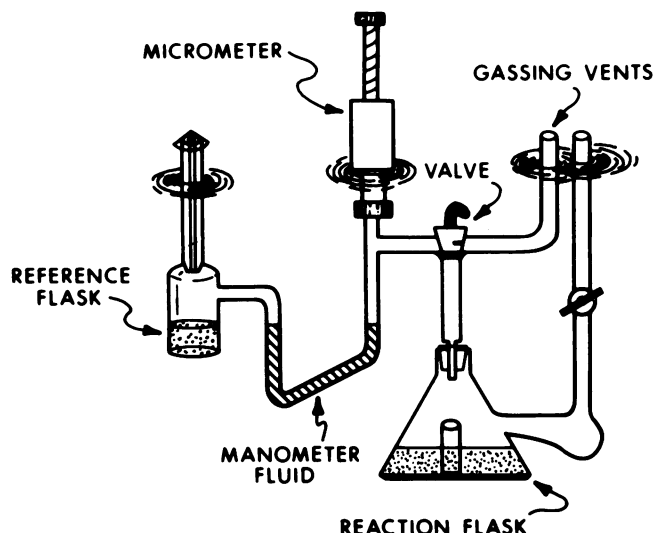


FIGURE 1. Warburg manometer fitted with center well flask. The tissue slices are incubated in the outer well of the flask, while the center well contains  $\text{CO}_2$  absorbent.

original headspace gas (24). The flask should then be closed, checked for leaks, and temperature allowed to equilibrate while shaking for an additional period before  $\dot{Q}_{\text{O}_2}$  measurements commence.

## Polarographic

Polarographic measurements of dissolved oxygen concentrations and tissue oxygen consumption involve the use of a glass-encased platinum or silver Clark-type electrode covered with an oxygen permeable cellophane membrane. With an appropriate applied voltage, a Clark electrode will produce a current linearly related to solution oxygen tension. Clark electrodes may be used in conjunction with waterjacketed cells having reaction volumes as small as 0.5 mL, allowing sensitive oxygen consumption measurements when using small amounts of tissue (Fig. 2). An added advantage to using a polarograph for tissue oxygen consumption measurements is that the  $P_{\text{O}_2}$  of the incubation medium is always known. This assures that a fall in  $P_{\text{O}_2}$  below a critical value will not result in erroneous measurements of  $\dot{Q}_{\text{O}_2}$ . The polarograph is adjusted by calibrating the electrode output to a recorder; this is done by zeroing with 100% nitrogen-saturated incubation buffer and then calibrating the recorder full-scale deflection with buffer saturated with a known oxygen concentration. Table 3 contains factors for calculating oxygen uptake in terms of microliters and nanomoles, since a polarograph differentiates only the percent oxygen saturation of a solution.

We have found that polarographic measurements of lung tissue slice oxygen consumption compare well with manometer-derived values (Table 2). Tissue slice oxygen consumption is linearly related to the wet weight of the tissue added to the polarograph cell, ranging from total lung slice weights of 20 to 75 mg, when analyzed in a 1.5-mL waterjacketed cell in 95% oxygen saturated buffer. We routinely measure  $\dot{Q}_{\text{O}_2}$  of three to four small 1-mm thick lung slices totaling approximately 40 mg wet weight. Oxygen consumption measurements are

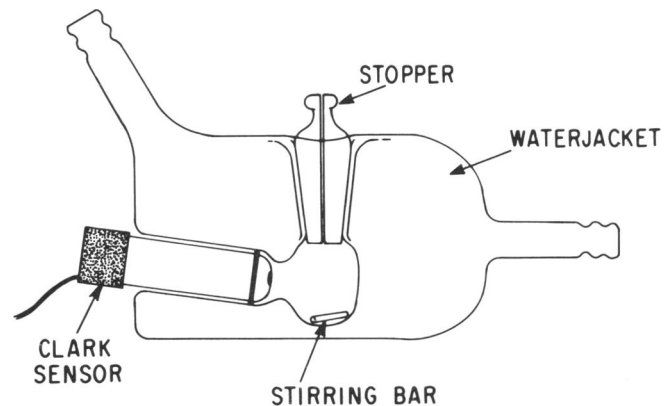


FIGURE 2. Polarograph cell and electrode used for oxygen consumption measurement. Biological material in the cell can have substrates or inhibitors added through the center hole stopper.

optimal when the oxygen saturation of the buffer is 40 to 60% or greater (Table 2) and when a spinbar maintains adequate gas mixing in the bulk phase of the incubation medium by rotating at 2 to 3 revolutions/sec.

## Summary of Lung Slice Oxygen Consumption Measurements

Lung tissue accounts for approximately 1% of total body oxygen consumption (25), and in rat lung tissue slices, has a lower  $\dot{Q}_{O_2}$  per gram of tissue than kidney, heart, liver and brain. This is likely due to the greater proportion of metabolically inactive structural elements present in lung tissue as opposed to other organs.

Lung tissue slice  $\dot{Q}_{O_2}$  values reported in the literature are quite variable, ranging for rats from approximately 0.7  $\mu\text{mole/min}$  per lung (26) to 2.0  $\mu\text{mole/min}$  per lung (12). Smaller mammals such as mouse, rat, guinea pig and rabbit have a greater  $\dot{Q}_{O_2}$  relative to tissue mass as opposed to lungs of larger animals including dogs, sheep and horses (27). This is due to both smaller animals having a greater tissue density of mitochondria, and larger animals having a greater proportion of metabolically inactive connective tissue (28).

The  $\dot{Q}_{O_2}$  of lung homogenates is considerably lower than when measured in more structurally intact lung tissue such as slices. This is due to the homogenization-induced release of nicotinamide dinucleotide nucleosidase activity (NADase), which hydrolyzes a reduced cofactor critical for mitochondrial oxidative metabolism (4,29). Rat lung homogenates fortified with 1.0 mM NADH have a  $\dot{Q}_{O_2}$  three to five times as great as a fresh homogenate metabolizing endogenous substrates. In an NADH-supplemented homogenate, we have measured a  $\dot{Q}_{O_2}$  of  $1.03 \pm 0.08 \mu\text{mole } O_2/\text{min}$  per rat lung ( $n = 5$ ,  $\pm$  SEM, 300–350 g rats), which is 60% less than measured in lung slices (Table 2). This suggests that in addition to the enhancement of NAD(H) breakdown by NADase, homogenization has other damaging effects on lung respiratory processes. It is interesting to note that the  $\dot{Q}_{O_2}$  of lung homogenates is maximal even at a low oxygen concentration of 5% ( $1.05 \pm 0.99 \mu\text{mole } O_2/\text{min}$  per rat lung), reconfirming that mitochondrial cytochrome oxidase has a low  $K_m$  for oxygen (30). Respiration in lung homogenates is maximal at 5% oxygen, while tissue slices do not achieve optimum  $\dot{Q}_{O_2}$  until 40 to 60% oxygen (Table 2), stressing the fact that oxygen diffusion through a tissue slice can limit respiration below a critical  $P_{O_2}$ .

Various biochemical reactions are responsible for lung  $O_2$  uptake, with mitochondrial electron transfer to molecular oxygen, forming  $2H_2O$ , as the quantitatively most significant. This reaction is cyanide sensitive, and from Table 2 it can be seen that cyanide-sensitive respiration accounts for about 85% of lung oxygen consumption. The remaining oxygen-consuming reactions in the lung can involve incorporation of oxygen

into substrates. For example, oxygen transferases are involved in catalyzing lung prostaglandin synthesis while hydroxylation of drugs and natural products can occur via mixed-function oxidases found in lungs. Pulmonary oxidative deamination is involved in systemic serotonin and norepinephrine metabolism. All of these reactions involve the production of oxygen-containing products. Also, the generation of potentially toxic partially reduced species of oxygen such as superoxide ( $O_2^-$ ), hydrogen peroxide ( $H_2O_2$ ), hydroxyl radical ( $OH^\bullet$ ) and singlet oxygen ( $^1O_2$ ) is a cyanide-insensitive process which occurs in lungs and consumes oxygen. These species of oxygen can be produced by soluble enzymes and by both mitochondrial and microsomal electron transport processes (18). All of these enzymatically catalyzed reactions and autooxidations contribute to lung tissue oxygen consumption which is not a mitochondrial electron transfer.

## Intermediary Metabolism in Lung Tissue Slices

In addition to the lungs' primary role in gas exchange, this organ utilizes energy in order to maintain structural and functional integrity. The metabolic processes of the lung are also critical for the maintenance of physiologic homeostasis. For example, the pulmonary release or modification of peptides, amines and prostaglandins plays an integral role in controlling vascular resistance and inflammatory reactions. Since other papers in this issue are devoted to a detailed discussion of particular metabolic processes of the lung, this section will discuss only those to which lung slice studies lend a particular insight.

When studying the kinetics of substrate utilization or product formation in tissue slices using radioisotope precursors, the concentration of both nonradioactive and radiolabeled metabolites of interest need to be determined in the tissue, so that valid rates of enzyme system activity can be measured. Before rates of product formation or substrate utilization can be determined, tissue pools of nonradioactive metabolic intermediates also must become equilibrated with products of the radiolabeled substrate. Times required for equilibration of substrate with intermediate range from minutes for molecules—such as glucose (1)—which are rapidly turned over, to hours for slowly turned over phospholipids (31). Also, in order to confirm that steady-state kinetics exist, it must be established that rates of substrate incorporation and production formation are linear with respect to time. Then, if product pool sizes can be quantitated and the isotope specific activities of the substrate and product are known, actual rates of product formation can be calculated.

Lung tissue slices have been used extensively in the study of lung phospholipid metabolism. This includes investigations of the incorporation of radiolabeled fatty

acids, glycerol and choline into various lipids (9,31,32). Also, the secretion of phospholipids into the alveolar space has been studied in lung slices (7).

Carbohydrate oxidation has also been studied in lung tissue slices. The relative activities of glycolysis and tricarboxylic acid metabolism versus the pentose phosphate shunt have been described by various investigators in both normal (1) and injured lung tissue (33). These experiments often involve the measurement of  $^{14}\text{CO}_2$  evolved from glucose labeled in the C-6 and C-1 positions and the quantitation of intermediates such as lactate. In normal lung, about 17% of added glucose is metabolized via the pentose phosphate shunt ( $^{14}\text{CO}_2$  released from 1- $^{14}\text{C}$ -glucose) and 83% of the glucose is utilized by other pathways ( $^{14}\text{CO}_2$  released from 6- $^{14}\text{C}$ -glucose).

Metabolic inhibitors may also be used to study the contribution of specific pathways to whole tissue slice metabolism. For example, KCN can be used to inhibit mitochondrial respiration. Then, any residual tissue slice oxygen consumption would represent alternative pathways of lung oxygen utilization (Tables 3 and 4).

## Lung Tissue Slices in Toxicological Studies

### Oxidant Air Pollutants

Photochemical air pollution contains many oxidizing gases including nitrogen oxides, peroxyacyl nitrates and ozone. Ozone has been extensively studied because it is a quantitatively more significant and toxic component of smog than nitrogen oxides and peroxyacyl nitrates (34).

NADH, NADPH and several amino acids including cysteine, tryptophan, methionine, tyrosine, histidine and phenylalanine will react with ozone. Ozone will react with free or esterified unsaturated fatty acids, producing potentially toxic byproducts such as hydrogen peroxide, malonaldehyde and other carbonyl compounds (35). Ozone is also capable of crossing cell membranes and reacting with cytoplasmic contents (36).

Extensive ozone inhalation studies with rodents and primates have shown the terminal and respiratory bronchiolar epithelium and alveolar Type I epithelial

**Table 4. Effect of oxygen concentration on cyanide-resistant respiration in rat lung tissue slices.<sup>a</sup>**

Oxygen concentration during $\dot{Q}_{\text{O}_2}$ measurement, % <sup>b</sup>	$\dot{Q}_{\text{O}_2}$ (+ CN), nmole/min per lung
5	0
15	70
20	110
40	170
60	240
75	280
85	320
95	390

<sup>a</sup> Tissue slice respiration was measured polarographically at the noted oxygen concentrations.

<sup>b</sup>  $\dot{Q}_{\text{O}_2}$  was measured in lung slices treated with 1 mM CN.

cells especially susceptible to damage (37). Alveolar macrophages are also found at sites of airway epithelial cell damage (38). Evaluation of both toxic reactions of ozone and the adaptive processes which occur in lungs either during, or subsequent to, ozone exposure are complicated by a variety of pulmonary responses to ozone, including edema, activation and infiltration of inflammatory cells, and proliferation of specific undamaged cells and organelles. Nevertheless, studies with lung tissue slices from rats following exposure to ozone have lent insight into mechanisms of toxicity and the structural-function alterations which might result in the lung.

Short-term acute exposure (2–4 ppm for less than 8 hr) of rats to ozone initially results in a 25% decrease in lung mitochondrial oxidative metabolism (39). Within 12 hr after exposure, the control  $\dot{Q}_{\text{O}_2}$  was attained, and 2 days after exposure, a peak rate of lung  $\dot{Q}_{\text{O}_2}$  stimulation (50% greater than controls) occurred. In the ozone-exposed rat lung,  $\dot{Q}_{\text{O}_2}$  remains elevated for several days after exposure, and by 21 days after exposure is 15% greater than controls. These observations were initially made using lung homogenates (40), and later confirmed in tissue slices (41). As mentioned previously, the  $\dot{Q}_{\text{O}_2}$  of lung homogenates supplemented with mitochondrial substrates was significantly less than lung  $\dot{Q}_{\text{O}_2}$  measured using tissue slices. The enhanced mitochondrial respiration in ozone-exposed lung slices is due to a concomitant increase in numbers of mitochondria present in lungs of rats recovering from ozone exposure (40), and not a consequence of stimulation of the respiratory activity of individual mitochondria. In fact, ozone initially depresses respiration of isolated lung mitochondria (41). Whether the size of the mitochondria was altered by ozone was not reported.

Chronic exposure of rats to ozone (0.8 ppm for 4 days) and nitrogen dioxide (5 ppm for 7 days) results in a similar increase in lung  $\dot{Q}_{\text{O}_2}$  (42) measured using tissue slices. Both of these exposure regimens also result in a stimulation of lung tissue slice glucose consumption, pyruvate production and lactate production (42). Morphologic studies show that hyperplasia occurs following

**Table 3. Oxygen content of Ringer's solutions equilibrated with 100% oxygen<sup>a</sup>.**

Temperature, °C	Unit	Value
25	$\mu\text{L/mL}$	28.2
	nmole/mL	1.26
	$\mu\text{g-atoms O}_2/\text{mL}$	2.54
37	$\mu\text{L/mL}$	23.9
	nmole/mL	1.07
	$\mu\text{g-atoms O}_2/\text{mL}$	2.14

<sup>a</sup>Calculated from data of Umbreit et al. (16).

oxidant air pollutant exposure (37,38). The increases in mitochondrial respiration and glucose consumption measured in lung tissue slices following inhalation of nitrogen dioxide and ozone reflect both the increased cellularity of the lung and the operation of energy-dependent reparative processes. Care must be taken when expressing and interpreting data from lungs which have been exposed to edemagenic compounds, since 100 mg of edematous lung tissue contains less metabolically active tissue than the same weight of lung derived from a control rat.

## Oxygen Toxicity

Pulmonary toxicity has long been known to be a consequence of breathing above-ambient concentrations of oxygen. The use of oxygen-enriched inspired air to treat hypoxemia during inpatient hospital therapy frequently results in toxic side effects. Although oxygen can be toxic to other organs, lungs are the most susceptible organ since blood oxygen content will not increase significantly, even during inhalation of oxygen-enriched gas. Oxygen toxicity can ultimately result in tracheobronchitis, adult respiratory distress syndrome and/or bronchopulmonary dysplasia (43). Recovery from oxygen poisoning or long-term exposure to sublethal oxygen concentrations may be associated with chronic pulmonary fibrosis.

It is likely that superoxide or secondary oxygen radicals are the deleterious agents in oxygen toxicity (18), and direct measurements relating hyperoxia with an increased pulmonary production of oxygen radicals have recently been made (44). There are many biological sources of superoxide, whose relative quantitative significance are unknown. These sources include phagocytes, soluble enzymes and autooxidizable components of electron transport processes (44).

Most nonenzymatic sources of cellular superoxide production should display first-order kinetics with respect to oxygen concentration, suggesting that hyperoxia inevitably leads to an increased intracellular production of oxygen radicals. We have examined CN-resistant respiration in rat lung tissue slices as a function of  $P_{O_2}$ , in order to better define the relationship between intracellular  $P_{O_2}$  and oxygen radical production. Polarographic measurements of tissue slice oxygen consumption in the presence of 1 mM CN reflects oxygen-consuming processes in the absence of mitochondrial respiration, which is quantitatively the most significant (Table 2). Many of these cyanide resistant forms of oxygen consumption involve production of potentially toxic superoxide anion and hydrogen peroxide, which in turn can react to produce singlet oxygen ( $^1O_2$ ) or hydroxyl radical ( $OH\cdot$ ). Table 4 shows that lung slice CN-resistant oxygen consumption is a function of oxygen concentration, even above 40%  $O_2$ , where, in 1-mm thick tissue slices, oxygen diffusion is known to no longer limit mitochondrial respiration (Table 2). The

slight increase in total lung slice  $\dot{Q}_{O_2}$  from 40% to 95%  $O_2$  (Table 2) may be due to increases in the CN-resistant component of lung respiration caused by increasing the  $P_{O_2}$ .

Morphometric studies have shown that hyperoxia also induces both hyperplasia and hypertrophic response in lungs (45), resulting in almost a doubling of cell numbers in the alveolar region of rat lungs following inhalation of 85%  $O_2$  for 7 days. These changes are reflected in an increase in whole rat lung  $\dot{Q}_{O_2}$  measured in tissue slices following *in vivo* exposure to oxygen (46) (Table 5). As with ozone-exposed rat lungs, this increase in  $\dot{Q}_{O_2}$  may reflect increases in metabolic processes which can support tissue reparative processes. Hypertrophy of mitochondria-rich lung cells, such as Type II pneumocytes and endothelial cells, following oxygen exposure may also contribute to the elevation in lung  $\dot{Q}_{O_2}$ . This can also account for the increase in recoverable mitochondria and measurable mitochondrial cytochrome oxidase activity from exposed rat lungs (Table 5).

Cyanide-resistant respiration measured in rat lung slices is directly related to the oxygen concentration in the incubation medium (Table 4). This suggests that the oxygen-consuming enzymatic and autooxidative processes measured in relatively intact lung tissue in the presence of CN are influenced by  $P_{O_2}$  and reflect the intracellular production of superoxide and hydrogen peroxide.

## Paraquat Toxicity

Paraquat (methyl viologen, 1,1'-dimethyl-4,4'-bipyridinium ion) is a broad-spectrum herbicide which is also toxic to man and animals. Mammalian toxicity is characterized by pulmonary edema which, after nonfatal doses, can progress to interstitial fibrosis (47). Paraquat primarily damages the lungs because there exists an oxygen- and energy-dependent mechanism for pulmonary paraquat accumulation (14). The lungs are

Table 5. Biochemical responses of rat lung tissue slices to hyperoxia.<sup>a</sup>

Measurement	Control rats	Exposed rats
$\dot{Q}_{O_2}$ , $\mu$ mole/min per rat lung	1.65 $\pm$ 0.10	3.21 $\pm$ 0.17
Mitochondrial protein isolated from rat lungs, mg	8.6 $\pm$ 1.1	13.7 $\pm$ 1.6
Units cytochrome oxidase activity of mitochondrial fraction <sup>b</sup>	0.096 $\pm$ 0.007	0.152 $\pm$ 0.015
Units of cytochrome oxidase activity of lung homogenate	0.369 $\pm$ 0.012	0.691 $\pm$ 0.34
Recovery of mitochondria from rat lungs, %	26	22

<sup>a</sup>Mean  $\pm$  SEM,  $n = 7$ ; rats were exposed to 85% oxygen for 7 days.

<sup>b</sup>1 U = 1  $\mu$ mole/min product formed.

also especially sensitive to paraquat because they experience a greater oxygen tension than other organs, and oxygen is a necessary reactant in the formation of toxic oxygen free radicals by paraquat (48).

Paraquat is readily reduced to a monocationic radical which in turn reacts with oxygen to form superoxide. The intracellular reduction of paraquat is a consequence of the interaction of paraquat with cellular electron transport processes such as the NADPH-cytochrome c reductase system of the endoplasmic reticulum (15). In face of constant intracellular redox cycling, minute quantities of paraquat can generate superoxide for extended periods of time.

When incubated with rabbit lung tissue slices, paraquat initially increases  $^{14}\text{CO}_2$  evolution from both 1- $^{14}\text{C}$ -glucose and 6- $^{14}\text{C}$ -glucose. After 2 to 3 hr,  $^{14}\text{CO}_2$  evolution then decreases back to or below control levels depending on dose. In 95% oxygen rather than 20% oxygen, paraquat has an even greater stimulatory effect of  $^{14}\text{CO}_2$  evolution from 1- $^{14}\text{C}$ -glucose and 6- $^{14}\text{C}$ -glucose (49). This suggests that paraquat has a stimulatory effect on both lung pentose phosphate and tricarboxylic acid pathways. Twenty percent oxygen may also have an inhibitory effect on tissue slice carbohydrate metabolism since we show that respiration is suboptimal at this oxygen concentration (Table 3). In rabbit lung tissue slices, paraquat also increases CN-resistant respiration in a dose and oxygen concentration-dependent manner (50). This indirect measurement of oxygen radical production suggests that paraquat is indeed increasing the generation of oxygen radicals in lung tissue.

Under normoxic conditions, paraquat has an inhibitory effect on rabbit lung slice oxygen consumption, either in the presence or absence of 10 mM glucose (51). When incubated in 95%  $\text{O}_2$ , the inhibitory effect of paraquat on tissue slice respiration is potentiated. This implies that both an increased intracellular reductive state (due to glucose addition) and an elevation of intracellular  $P_{\text{O}_2}$  will significantly stimulate the generation of superoxide by reduced paraquat. Hyperoxia has no effect on the ability of lung slices to accumulate paraquat, while hypoxic conditions inhibit paraquat uptake in rat lung slices (14). This observation may also help explain the mechanism by which hypoxia limits paraquat toxicity (52).

## Conclusions

Lung tissue slices have proved useful in the study of lung metabolism and toxicology. Lung slices, which are simple to prepare in large numbers, are invaluable for metabolic and dose-response studies in tissue from either the same animal or a number of animals. Lung slices also lend themselves to an *in vitro* study of *in vivo*-induced changes. Mechanistic studies of metabolic processes in a complex tissue are also possible, providing investigators with a useful tool which can have widespread applications in studies of lung metabolism.

This report has been reviewed by the Health Effects Research Laboratory, U.S. Environmental Protection Agency and approved for publication. Mention of trade names or commercial products does not constitute endorsement or recommendation of use.

## REFERENCES

1. O'Neil, J. J., and Tierney, D. F. Rat lung metabolism: glucose utilization by isolated perfused lungs and tissue slices. *Am. J. Physiol.* 226: 867-873 (1974).
2. Henney, C. S. Cell-mediated immune reactions in the lung. In: *Immunologic and Infectious Reactions in the Lung* (C. H. Kirkpatrick and H. Y. Reynolds, Eds.), Marcel Dekker, New York, 1976, p. 59.
3. Bhatnagar, R. S., Hussain, M. Z., and Belton, J. C. Applications of lung organ culture in environmental investigations. In: *Assessing Toxic Effects of Environmental Pollutants* (S. D. Lee, Ed.), Ann Arbor Science Publishers Inc., Ann Arbor, MI, 1979, p. 121.
4. Barron, E. G. S., Miller, Z. B., and Bartlett, G. R. Studies of biological oxidations. XXI. The metabolism of lung as determined by study of slices and ground tissue. *J. Biol. Chem.* 171: 791-800 (1947).
5. O'Neil, J. J., Sanford, R. L., Wasserman, S., and Tierney, D. F. Metabolism in rat lung tissue slices: technical factors. *J. Appl. Physiol.* 43: 902-906 (1977).
6. Gregorio, C. A., and Massaro, D. Influence of insulin on amino acid uptake by lung slices. *J. Appl. Physiol.* 42: 216-220 (1977).
7. Marino, P. A., and Rooney, S. A. Surfactant secretion in a newborn rabbit lung slice model. *Biochim. Biophys. Acta* 620: 509-519 (1980).
8. Postlewait, E. M., Young, S. L., and Knelson, J. H. ATP in rat lung tissue. *Physiologist* 17: 310 (1974).
9. Epstein, M. F., and Farrell, P. M. The choline incorporation pathway: primary mechanism for de-novo lecithin synthesis in fetal primate lung. *Pediatr. Res.* 9: 658-665 (1975).
10. Krebs, H. A. Rate control of the tricarboxylic acid cycle. *Adv. Enzyme Regulation* 8: 335-353 (1970).
11. Stadie, W. C., and Riggs, B. C. Microtome for the preparation of tissue slices for metabolic studies of surviving tissues *in vitro*. *J. Biol. Chem.* 154: 687-690 (1944).
12. Levy, S. E., and Harvey, E. Effect of tissue slicing on rat lung metabolism. *J. Appl. Physiol.* 37: 239-240 (1974).
13. Scholz, R. W., and Rhoades, R. A. Lipid metabolism by rat lung *in vitro*. Effect of starvation and refeeding on utilization of [ $^{14}\text{C}$ ] glucose by lung slices. *Biochem. J.* 124: 257-264 (1971).
14. Montgomery, M. R., Wyatt, I., and Smith, L. L. Oxygen effects on metabolism and paraquat uptake in rat lung slices. *Exptl. Lung Res.* 1: 239-280 (1980).
15. Talcott, R. E., Shu, H., and Wei, E. T. Dissociation of microsomal oxygen reduction and lipid peroxidation with the electron acceptors paraquat and menadione. *Biochem. Pharmacol.* 28: 665-671 (1979).
16. Umbreit, W. W., Burris, R. H., and Stauffer, J. F. In: *Manometric and Biochemical Techniques*, 5th Ed. Burgess Publishing Co., Minneapolis, MN, 1972, pp. 1-147.
17. Engelbrecht, F. M., and Maritz, G. Influence of substrate composition on *in vitro* oxygen consumption of lung slices. *S. Afr. J. Lab. Clin. Med.* 20: 1882-1889 (1974).
18. McCord, J. M. Superoxide, superoxide dismutase and oxygen toxicity. In: *Reviews in Biochemical Toxicology* (E. Hodgson, J. R. Bend and R. M. Philpot, Eds.), Elsevier, New York, 1979.
19. Stroeve, P. Diffusion with irreversible chemical reaction in heterogeneous media: application to oxygen transport in respiring tissue. *Theor. Biol.* 64: 237-251 (1977).
20. Venkataraman, K., Wang, T., and Stroeve, P. Oxygen diffusion into heterogeneous tissue with combined oxygen consumption kinetics. *Ann. Biomed. Eng.* 8: 17-27 (1980).
21. Bryant, J. O., Akers, W. W., and Busch, A. W. Limitations of oxygen transfer in the Warburg apparatus. In: *Proceedings*, 22nd

- Annual Industrial Waste Conference, Purdue University, Lafayette, IN, 1968, pp. 686-698.
22. Olsen, D. B. Neuro-humoral hormonal secretory stimulation of pulmonary surfactant in the rat. *Physiologist* 15: 230 (1972).
  23. Oyarzun, J. M., and Clements, J. A. Ventilatory and cholinergic control of pulmonary surfactant in the rabbit. *J. Appl. Physiol.* 43: 39-45 (1977).
  24. Frazer, D. A., Baks, R. E., Lippmann, M., and Stokinger, H. E. Exposure Chambers for Research in Animal Inhalation. Public Health Service Publication No. 662, U.S. Government Printing Office, Washington, DC, 1959, p. 26.
  25. Fisher, A. B. Oxygen utilization and energy production. In: *The Biochemical Basis of Pulmonary Function* (R. G. Crystal, Ed.), Marcel Dekker, New York, 1978.
  26. Caldwell, P. R. B., and Wittenberg, B. A. The oxygen dependency of mammalian tissue. *Am. J. Med.* 57: 447-452 (1974).
  27. Krebs, H. A. Body size and tissue respiration. *Biochim. Biophys. Acta* 4: 249-269 (1950).
  28. Massaro, G. D., Gail, D. B., and Massaro, D. Lung oxygen consumption and mitochondria of alveolar epithelial and endothelial cells. *J. Appl. Physiol.* 38: 588-592 (1975).
  29. Bierkierkunst, A., Artman, M., and Silman, M. Tissue metabolism in infection: soluble nicotinamide-adenine dinucleotidase in organs from tuberculous mice. *Am. Rev. Respir. Dis.* 89: 575-578 (1964).
  30. Jobsis, F. F., and LaManna, J. C. Kinetic aspects of intracellular redox reactions: *in vivo* effects during and after hypoxia and ischemia. In: *Extrapulmonary Manifestations of Respiratory Disease* (E. D. Robin, Ed.), Marcel Dekker, New York, 1978, p. 63.
  31. Young, S. L., and Tierney, D. F. Dipalmitoyl lecithin secretion and metabolism by rat lung. *Am. J. Physiol.* 222: 1539-1544 (1972).
  32. Abe, N., Kasuyama, R., and Tierney, D. F. Utilization of palmitate and stearate in rat lung tissue slices and isolated perfused lung. *Am. Rev. Respir. Dis.* 115: 299-309 (1977).
  33. Young, S. L., O'Neil, J. J., Kasuyama, R. S., and Tierney, D. F. Glucose utilization by edematous rat lungs. *Lung* 157: 165-177 (1980).
  34. Hackney, J. D., Linn, W. S., Bell, K. A., and Buckley, R. D. Health effects of air pollution: controlled studies in humans. In: *Assessing Toxic Effects of Environmental Pollutants* (S. D. Lee and J. B. Mudd, Eds.), Ann Arbor Science Publishers Inc., Ann Arbor, MI, 1979, pp. 42-67.
  35. Mudd, J. B., and Freeman, B. A. Reaction of ozone with biological membranes. In: *Biochemical Effects of Environmental Pollutants* (S. D. Lee, Ed.), Ann Arbor Science Publishers Inc., Ann Arbor, MI, 1977, pp. 96-117.
  36. Freeman, B. A., Sharman, M. C., and Mudd, J. B. Reaction of ozone with phospholipid vesicles and human erythrocyte ghosts. *Arch. Biochem. Biophys.* 197: 264-272 (1979).
  37. Stephens, R. J., Sloan, M. F., Evans, M. J., and Freeman, G. Early response of lungs to low levels of ozone. *Am. J. Pathol.* 74: 31-42 (1974).
  38. Mellick, P. W., Dungworth, D. L., Schwartz, L. W., and Tyler, W. S. Short term morphologic effects of high ambient levels of ozone on lungs of rhesus monkeys. *Lab. Invest.* 36: 82-94 (1975).
  39. Mustafa, M. S., DeLucia, A., York, G. K., Arth, C., and Cross, C. E. Ozone interaction with rodent lung. II. Effects on oxygen consumption of mitochondria. *J. Lab. Clin. Med.* 82: 357-365 (1973).
  40. Mustafa, M. G., and Cross, C. E. Effects of short term ozone exposure on lung mitochondrial oxidative and energy metabolism. *Arch. Biochem. Biophys.* 162: 585-594 (1974).
  41. Mustafa, M. G., Hacker, A. D., Ospital, J. J., Hussain, M. Z., and Lee, S. D. Biochemical effects of environmental oxidant pollutants in animal lungs. In: *Biochemical Effects of Environmental Pollutants* (S. D. Lee, Ed.), Ann Arbor Science Publishers, Inc., Ann Arbor, MI, 1977, p. 59.
  42. Mustafa, M. G., and Lee, S. D. Biological effects of environmental pollutants: methods for assessing biochemical changes. In: *Assessing Toxic Effects of Environmental Pollutants* (S. D. Lee and J. B. Mudd, Eds.), Ann Arbor Science Publishers Inc., Ann Arbor, MI, 1979, p. 105.
  43. Frank, L., and Massaro, D. Oxygen toxicity. *Am. J. Med.* 69: 117-126 (1980).
  44. Freeman, B. A., and Crapo, J. D. Hyperoxia increases oxygen radical production in rat lungs and lung mitochondria. *J. Biol. Chem.* 256: 10986-10992 (1981).
  45. Crapo, J. D., Barry, B. E., Foscue, H. A., and Shelburne, J. Structural and biochemical changes in rat lungs occurring during exposures to lethal and adaptive doses of oxygen. *Am. Rev. Respir. Dis.* 122: 123-143 (1980).
  46. Gail, D. B., and Massaro, D. Oxygen consumption by rat lung after *in vivo* hyperoxia. *Am. Rev. Respir. Dis.* 113: 889-891 (1976).
  47. Haley, T. J. Review of the toxicology of paraquat. *Clin Toxicol.* 14: 1-46 (1979).
  48. Fridovich, I., and Hassan, H. M. Paraquat and the exacerbation of oxygen toxicity. *Trends Biochem. Sci.* 4: 113-115 (1979).
  49. Rossouw, D. J., and Engelbrecht, F. M. The effect of oxygen and paraquat on the <sup>14</sup>C-glucose oxidation of rabbit alveolar macrophages and lung slices. *South Afr. Med. J.* 55: 558-560 (1979).
  50. Rossouw, D. J., and Engelbrecht, F. M. The effect of paraquat on the aerobic metabolism of rabbit alveolar macrophages and lung fibroblasts. *South Afr. Med. J.* 55: 20-23 (1979).
  51. Rossouw, D. J., and Engelbrecht, F. M. The influence of paraquat on the *in vitro* oxygen consumption of rabbit lung. *South Afr. Med. J.* 54: 199-201 (1978).
  52. Rhodes, M. D. Hypoxic protection of paraquat poisoning: a model for respiratory distress syndrome. *Chest* 66: 341-342 (1974).